On self-organized criticality in nonconserving systems

J. E. S. Socolar* and G. Grinstein
IBM Research Division, Thomas J. Watson Research Center, P. O. Box 218, Yorktown Heights, New York 10598

C. Jayaprakash
Physics Department, Ohio State University, Columbus, Ohio 43210
(Received 22 April 1992)

Two models with nonconserving dynamics and slow continuous deterministic driving, a stick-slip model (SSM) of earthquake dynamics and a toy forest-fire model (FFM), have recently been argued to show numerical evidence of self-organized criticality (generic, scale-invariant steady states). To determine whether the observed criticality is indeed generic, we study these models as a function of a parameter γ which was implicitly tuned to a special value, $\gamma=1$, in their original definitions. In both cases, the maximum Lyapunov exponent vanishes at $\gamma=1$. We find that the FFM does not exhibit self-organized criticality for any γ, including $\gamma=1$; nor does the SSM with periodic boundary conditions. Both models show evidence of macroscopic periodic oscillations in time for some range of γ values. We suggest that such oscillations may provide a mechanism for the generation of scale-invariant structure in nonconserving systems, and, in particular, that they underlie the criticality previously observed in the SSM with open boundary conditions.

PACS number(s): 05.20.−y, 05.45.+b, 05.70.Jk, 64.60.−i

I. INTRODUCTION

It has recently been discovered that certain nonequilibrium model systems with local interactions evolve to a scale-invariant or "critical" steady state characterized by algebraic decays of correlations and a power-law distribution of the sizes of relaxation events [1]. In contrast to the situation in equilibrium systems, the critical state is achieved for generic values of the parameter of the system; no fine tuning is necessary. This phenomenon, termed self-organized criticality (SOC), has been conjectured to occur commonly in spatially extended, dissipative systems that are driven slowly relative to the system's relaxation rate [2]. It has been suggested [1] that SOC is responsible for the common occurrence of scale invariance in nature.

The term SOC applies to systems that are driven either completely deterministically at a very low rate, or by "slow noise"—random local perturbations, each of which is applied only after the system has relaxed fully in response to any prior perturbation. It is not at all clear that traditional analytical methods developed for equilibrium or noisy nonequilibrium problems can be applied to such systems. Nevertheless, the slow noise or deterministic chaotic fluctuations in the critical state might approximate white noise at some level, so analytical results for noisy systems may at least be taken as a useful guide in the study of SOC.

A fundamental result for driven nonequilibrium systems subject to external white noise is that scale invariance can indeed occur generically, but *only in systems with either a conservation law or a special continuous symmetry,* such as the translation invariance which allows even equilibrium interfaces to exhibit rough, scale-invariant phases [3]. The only exactly solved class of slow noise models—the "Abelian sandpile models" [4]—behave in a qualitatively similar manner: Dhar has demonstrated that these models exhibit critical correlations when the relaxational dynamics is conserving [4]. Moreover, straightforward application of the results of Ref. [4] shows that in the absence of conservation the Abelian models have exponentially decaying correlations under generic conditions. In light of these results, the well-established [1,5] occurrence of SOC in slowly driven, non-Abelian conserving model systems seem quite natural; but the recent discovery of deterministic (non-Abelian) models displaying SOC *without* a conserved quantity [6–8] is somewhat surprising and very intriguing, since it suggests a different mechanism for the generic generation of scale-invariant structure.

In this paper we focus on the problem of SOC in systems without a local conservation law. We study two (non-Abelian [9]) deterministic nonconserving models that have shown strong numerical evidence of SOC: a "forest-fire" model (FFM) that has been argued to produce structure reminiscent of turbulence [6], and a stick-slip model (SSM) of earthquake dynamics [8]. These two models (together with a model of friction [7] that is quite close to the SSM), are, to our knowledge, the only nonconserving systems in which plausible evidence for SOC has been found. Though they differ considerably in detail, the models share some basic features: In both cases, a real variable u_i is defined on the sites of a square lattice and all u_i are increased slowly and uniformly until one of them reaches a threshold value U. Upon reaching threshold, u_i "topples," decreasing by some amount, and "kicks" its near neighbors u_j, increasing each u_j by an amount that depends on u_i and/or u_j. This increase may

cause a neighbor to exceed U in which case it topples too, and a chain reaction or "avalanche" may ensue. (Explicit statements of the toppling and kicking rules are given in subsequent sections.) In both cases, the threshold dynamics imply that individual sites act as driven oscillators, ramping up to threshold (or possibly being kicked over), then dropping well below threshold, and ramping up again. Roughly speaking, the large avalanches which are characteristic of SOC occur when connected clusters of sites are in phase, so that when one reaches threshold the others are near enough to be kicked over threshold.

Our aim here is to determine whether SOC can be generic in such models and, if so, under what conditions. To that end, we introduce a parameter γ into the FFM and SSM and study its effects on their stable states [10]. In both models we find that $\gamma=1$ is a special point that separates two regimes of qualitatively different behavior. Interestingly, $\gamma=1$ is the value studied in the original SSM and one of the two values studied in the FFM.

Exploring the phenomenology of the systems for different values of γ, we identify regimes of strictly periodic states, wherein the value of every variable recurs after one period. We also find states wherein the individual variables fluctuate chaotically while the mean, or spatially averaged, variable appears to oscillate periodically or even chaotically in time. We call such states, which can be thought of as breaking a continuous time-translation symmetry, "periodic or chaotic in the mean," respectively, and suggest that they might provide a different mechanism for generating scale-invariant behavior under generic conditions.

A more detailed summary of our main results follows. Though previous studies of the FFM and SSM have, respectively, used periodic and open boundary conditions, here we consider periodic boundary conditions in both cases. The effects of more physical boundary conditions in the SSM may be important, but are best addressed after a proper understanding of the periodic boundary condition case is achieved. We comment on the effects of open boundaries in the SSM only in Sec. VI.

For the FFM, we find that SOC does not occur for any values of γ, including those for which it was previously claimed ($\gamma=1,2$). The periodic states for $\gamma\leq 1$ in the FFM, which have only system-wide avalanches, are completely characterized. The maximum Lyapunov exponent is negative (zero) for $\gamma<1$ ($\gamma=1$). Complex behavior—possibly states periodic in the mean—is observed for a small range of $\gamma>1$, but the avalanche-size distribution spectrum does not appear to be critical. Above this range we observe manifestly noncritical behavior, though at $\gamma=2$ the correlation length is quite long ($\xi\sim 50$).

For the SSM with periodic boundary conditions, we also show that SOC does not occur for any γ. For $\gamma<1$ we find only strictly periodic states with negative maximum Lyapunov exponents, the avalanche spectrum being dominated by small events. For $\gamma>1$ the most commonly occurring states are also strictly periodic, with negative maximum Lyapunov exponents, but they exhibit avalanches comparable to the system size. We have also observed some states that appear not to be strictly periodic. The avalanche spectra in these rare states are almost identical to those of the periodic states for $\gamma>1$ in that only a few different avalanche sizes occur. We also demonstrate that $\gamma=1$ is a unique point at which the maximum Lyapunov exponent of each stable state vanishes; all the states are strictly periodic and exactly one site topples in each avalanche.

In Secs. II and III we discuss some general issues relevant to the interpretation of numerical results and the identification of SOC. In Secs. IV and V we present results for the FFM and SSM, respectively, and in Sec. VI we speculate about the effects of open boundary conditions and possible mechanisms for the generation of scale invariance in generic nonconserving systems.

II. PERIODIC STATES AND SOC

Since the time evolution of the individual variables in the models studied here is basically periodic, it is not surprising that periodic states occur frequently. We have already pointed out that these states are of two different types: strictly periodic states (hereafter referred to simply as periodic), and states "periodic in the mean," with local chaotic fluctuations, but wherein the spatial average executes periodic oscillations for large L. Both types of states are familiar from other extended nonequilibrium systems [11] such as coupled map lattices [12]. The absence of fluctuations makes the former group less interesting conceptually, though in practice (see Sec. V) periods can become extremely long and the spatial structure extremely complex. In principle these states might even have avalanche-size distribution functions with power-law tails. One might call such behavior SOC, but this is quite different from the original conception of the term, which refers to states with nontrivial fluctuations.

The second group of periodic states do have such fluctuations. They can be thought of as breaking a continuous symmetry—time-translation invariance—and so might be expected to exhibit, in analogy with the breaking of a continuous symmetry in noisy systems, power-law decays of correlations associated with the resulting Goldstone mode [13–15]. Since such symmetry breaking can occur generically, this represents another potential mechanism for producing power laws in slowly driven systems without fine tuning, though, again, a different one than in the original notion of SOC, which makes no reference to symmetry breaking or temporal periodicity. One should also be alert to the possibility, especially in two-dimensions (2D), of "quasiordered" nearly periodic states which, in analogy to the Kosterlitz-Thouless phases familiar from equilibrium 2D XY models [16], do not break time-translation symmetry but exhibit power-law decays of correlations as a consequence of almost doing so.

To find SOC as originally envisaged, i.e., generic, scale-invariant states without symmetry breaking, one must clearly look in the chaotic regime, chaos being the only available source of fluctuations. (It is possible that such critical states occur with only "weak chaos"—a maximum Lyapunov exponent λ of zero and power-law spreading of trajectories—but $\lambda=0$ occurs only at the

special point $\gamma=1$ in the models studied here, and not generically [17].) As discussed in Secs. IV and V, however, we find no evidence of such "conventional" SOC behavior for the models under study when periodic boundary conditions are applied. The SSM with open boundary conditions is briefly discussed in Sec. VI.

III. IDENTIFYING SOC

A. Avalanche-size distribution $P(s)$

The most familiar diagnostic for determining whether or not slowly driven systems exhibit SOC is the distribution of avalanche sizes $P(s)$ [1]. Power-law decay of this quantity, i.e., $P(s)\sim s^{-\beta}$ out to a finite-size cutoff $s^*(L)$, which grows algebraically with L, $s^*(L)\sim L^{\nu}$, [18], is the typical signature of SOC. Owing to computational limits it can of course be difficult to distinguish true algebraic decays from exponential behavior, e.g., $s^{-\beta}e^{-s/s_0}$, when the characteristic avalanche size s_0 is large.

As we shall see, the stable states in the FFM and SSM have a variety of different avalanche-size spectra, ranging from only single-site avalanches or only avalanches of size L^2, to complicated spectra corresponding to many distinct avalanche sizes.

B. "Susceptibility" χ and maximum Lyapunov exponent λ

In addition to $P(s)$, several other measures of collective behavior are useful in understanding the properties of the models. The most direct is an analog of the order-parameter susceptibility in equilibrium systems: the sum over all sites of the equal-time correlation function

$$\chi\equiv\sum_{i,j}G_c(i,j)/N\ , \tag{1}$$

where

$$G_c(i,j)\equiv\langle u_iu_j\rangle-\langle u_i\rangle\langle u_j\rangle\ . \tag{2}$$

Here $N\equiv L^d$ is the number of sites of the system in d dimensions and $\langle\ \rangle$ denotes an average over time. For the time averaging, we consider the variables to increase at a fixed rate during continuous driving and average over the continuous-time variable. The avalanches are considered instantaneous on this time scale, so configurations that occur during an avalanche do not enter the average.

The quantity χ is a familiar measure of criticality in equilibrium, typically diverging with N at a continuous phase transition. It is, however, a useful diagnostic only when the system tends to order in a spatially uniform manner, i.e., at wave vector $\mathbf{q}=\mathbf{0}$. If the ordering occurs at nonzero $\mathbf{q}$, as in antiferromagnets, then χ typically remains finite, and one needs to study the appropriate finite-q susceptibility to hope to see a divergence with N. Even with ordering at $\mathbf{q}=\mathbf{0}$, χ is useful only if G_c decays sufficiently slowly with r, the separation between site i and j, at the putative critical point: If $G_c\sim r^{-\eta}$ at large r, then χ diverges (like $L^{d-\eta}$) only if $\eta\le d$. In the complex nonequilibrium systems considered here it is not at all clear *a priori* whether algebraic correlations tend to develop only at $\mathbf{q}=\mathbf{0}$, that if so they decay slowly enough for χ to diverge, or even that the correlations tend to be homogeneous rather than varying randomly in space, as in a spin glass [19]. Correlations in the FFM and SSM, however, behave "ferromagnetically," with $G_c>0$ for all r and all parameter values we checked. Moreover, for parameters where χ saturates with increasing L, data for G_c show no evidence of a decay with a large power of r. Thus the divergence of χ with L is a reliable indicator of the presence of critical behavior or ordering in these models and the saturation of χ with increasing L indicates noncritical behavior.

Writing χ in the form $\chi=N(\langle M^2\rangle-\langle M\rangle^2)$, where M is the spatial average $\sum_i u_i/N$, makes it clear that in either kind of periodic state (or in states where M fluctuates chaotically in time in the large-N limit), χ diverges linearly with N. This provides a useful tool for distinguishing such states from ones in which M is constant in time for large N, the divergence of χ in the latter being sublinear in N.

Further insight about the state and fluctuations of the system is provided by the maximum Lyapunov exponent λ, whose positivity is taken here as the definition of chaos, and whose vanishing signals the onset of chaotic behavior.

IV. FOREST-FIRE MODELS

A. Definition

The forest-fire or "epidemic" model studied here is a generalization of the deterministic model with periodic boundary and random initial conditions introduced in Ref. [6]. The variable $u_i(\tau)$ assumes values between 0 and 4, and represents the height of a tree on site i of a square $L\times L$ lattice at (discrete) time τ. For $u_i(\tau)\ge 2$, $1\le u_i(\tau)<2$, or $0\le u_i<1$, the tree is said to be on fire, living, or ash, respectively. Trees evolve under simultaneous updating according to the following rules.

(i) Any tree not on fire grows by a small amount p at each time step: $u_i(\tau+1)=u_i(\tau)+p$, unless (ii) it is living and has at least one nearest neighbor on fire, in which case it "catches fire" (is "kicked"), i.e., $u_i(\tau+1)=\gamma[u_i(\tau)-1]+2$. (iii) A tree on fire burns ("topples") in one time step: $u_i(\tau+1)=u_i(\tau)-2$.

Rule (ii) makes clear that γ controls the rate at which nearby trajectories converge ($\gamma<1$) or diverge ($\gamma>1$). The original model was discussed only for $\gamma=1$, the boundary between these two regimes, and $\gamma=2$, and for $p>0$, criticality at $p=0$ being inferred from numerical results obtained for p's down to about 0.001. Following Ref. [7] we study the model directly in the $p=0$ limit, where the driving or growth is infinitely slow relative to the spread and burning of fires. In this limit, fires propagate according to rules (ii) and (iii), until no fire remains on the lattice. At the next time step, which represents the infinitely slow growth of the entire forest, the largest variable u_I is identified, and all variables are increased by $2-u_I$, i.e., by the amount required for u_I to catch fire spontaneously. The spread of this fire then occurs through rules (ii) and (iii), and so on. Unlike for finite p, where some fraction of sites is on fire at any given time,

the $p=0$ limit has discrete fires ("avalanches") of finite size and duration.

B. Previous results for $p>0$

Most of the reported results [6] for the continuous-variable FFM at nonzero p have been obtained for 2D and $\gamma=2$, though similar behavior is reported [6,20] for $\gamma=1$. Snapshots of the lattice typically consist of rather straight, linear fire fronts, separated by a distance of $O(1/p)$, sweeping across the lattice with unit speed, consuming living trees, and leaving ash in their wake. The lengths of these fronts seem also to grow like $\xi\approx 1/p$ for p's down to roughly 0.001. Since the fronts are nearly straight, the fractal dimension of the fires out to distances of $O(\xi)$ is found to be very nearly unity; at larger distances it crosses over to the expected value of 2. The presumption has been that ξ diverges in the $p=0$ limit, thereby demonstrating the occurrence of SOC. Since the trees grow at rate p, the fundamental cycle time of the system scales like $1/p$. Steady state is achieved only after many cycles, so as p decreases, one must not only look at larger and larger systems to see that ξ is continuing to increase, but wait longer and longer. These considerations have hitherto restricted study to $p>0.001$.

C. Absence of SOC at $p=0$

We now argue that for neither $\gamma=1$ nor $\gamma=2$ is the FFM truly critical in the $p=0$ limit. At sufficiently small p, ξ in fact saturates at some finite value. Indeed, over the whole range of γ's we studied, $0<\gamma\leq 2$, the only hint of potential criticality occurs for γ just above 1, $1<\gamma<1.2$, say, where quasiordered periodic states are a possibility. A summary of our numerical results in the various ranges of γ values follows. Here a cycle is defined as the phase-space trajectory of the system between topplings of a designated site, and λ is measured by the decay of $\sum_i |u_i(n)-v_i(n)|$, where n counts the cycles and $v_i(0)=u_i(0)+\epsilon_i$ with small random ϵ_i. The period T of a periodic state is given in units of cycles. (For the periodic boundary conditions considered here, T is independent of the choice of the designated site and is, on average, linearly related to the continuous time variable.)

$0<\gamma<1$: For $\gamma<1$ only periodic states occur, consistent with expectations based on the convergence of nearly trajectories. In these states, $u_i>1$ for all i at the beginning of each avalanche. Thus every tree burns to ash, $u_i<1$, in each avalanche, so each avalanche constitutes one cycle and has size L^2. Hence $\chi\sim L^2$ and $P(s)=\delta_{s,L^2}$. The period $T=L^2$, since each of the L^2 sites precipitates exactly one avalanche before a given configuration of values recurs. For each L, the set of values of u_i immediately after an avalanche is invariant. Given that at some time all sites fall in the same avalanche, it can be shown that the system will converge to a state in which $\{u_i\}=\{(\gamma-\gamma^n)/(1-\gamma^{L^2})$; $n=1,\ldots,L^2\}$. Given that every site topples in every avalanche, however, it is clear that arbitrary permutation of the u_i values produces an essentially equivalent periodic state; different initial conditions lead to different permutations. These states have $\lambda<0$. (See Fig. 1).

$\gamma=1$: For $\gamma=1$ the same kind of states occur, the only difference being that the values of the u_i attained in a period are no longer unique: small changes in initial conditions produce small changes in these values, implying $\lambda=0$. Other, more complex, periodic states with avalanches smaller than L^2 and a less trivial avalanche distribution function also occur for $\gamma=1$. These states also have $\lambda=0$.

$1<\gamma<\gamma^*\approx 1.2$: For γ's slightly larger than 1, the model is no longer perfectly periodic, but shows the expected chaotic fluctuations associated with trajectory spreading: $\lambda>0$. (See Fig. 1.) As can be seen in Fig. 2, for a given γ between 1 and 1.2 there are two distinct regimes of rapid growth of χ. These correspond to two different types of states, each with macroscopic oscillations of the average variable $M(t)$. (See Fig. 3.) In neither of these states does the avalanche distribution show any obvious sign of scale invariance. For smaller L's, $P(s)$ is rather flat out to sizes s of $O(L^2)$, where it has two pronounced peaks reminiscent both of the δ_{s,L^2} spikes seen for $\gamma<1$ and the "great events" peaks observed in various other simple earthquake and sandpile models [21]. [See Fig. 4(a).] For larger systems, the two peaks disappear and $P(s)$ appears to decay exponentially beyond some relatively large size. [See Fig. 4(b).] The crossover in L from the peaked distribution to the exponential one coincides with the flat feature in $\chi(L)$ in Fig. 2. It remains unclear whether oscillations in the mean (and the concomitant growth of χ like L^2) persist for larger L, or whether, as for $\gamma>\gamma^*$ (discussed below), the state is actually time-translation symmetric with a rather long correlation length. To understand the significance and value of γ^*, one must consider how states with appropriate distributions of u_i's evolve for two cycles. One finds that distributions with $0<u_i<b$ for all i, with $b=(\gamma^3-1)(\gamma-1)$, can satisfy the same condition after two cycles and thereby produce stable oscillations, provided that $b<1-1/\gamma$. The states represented in Fig. 3 are closely approximated by such a description. The maximum value of γ for which this type of state can be stable therefore satisfies $\gamma^4-\gamma=1$, yield-

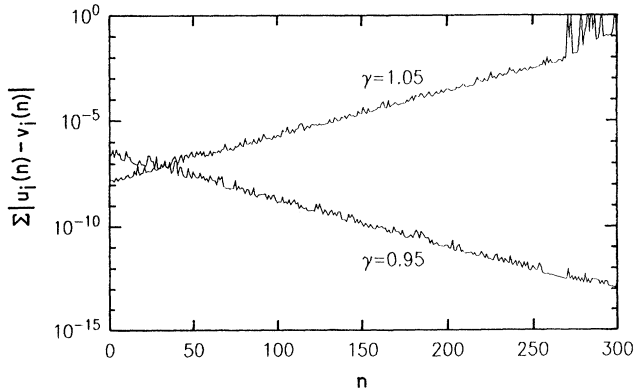

FIG. 1. Trajectory convergence (divergence) for the FFM with $\gamma=0.95$ (1.05) and $L=32$. The random perturbation is applied at $n=0$, after a transient of 10 (1000) cycles.

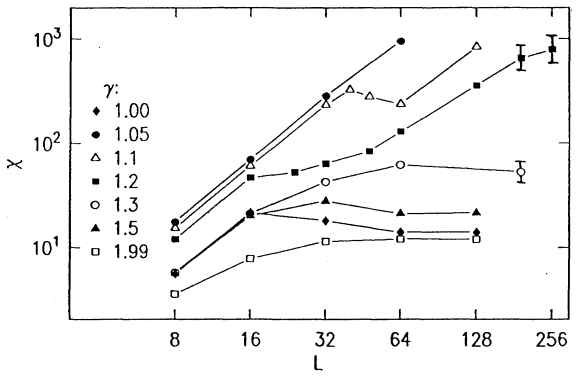

FIG. 2. Susceptibilities for the FFM with $\gamma \geq 1$. All runs with $L \leq 128$ included 10^4 cycles after a transient of 10^4 cycles. Runs with $L \geq 192$ included 10^3 cycles after a transient of 10^3 cycles and hence are less reliable. Error bars are rough estimates based on only a few runs with different initial conditions; when not explicitly shown they are approximately equal to the size of the symbols. Note the difference between $\gamma = 1.2$ and 1.3 at the larger values of L. Note also the drastic difference between $\gamma = 1.05$ and 1.00. The crossover between the two ordered states (see text) is most apparent at $\gamma = 1.1$.

ing $\gamma^* \approx 1.22$. This accounts for the change in behavior above $\gamma \approx 1.2$ visible in Fig. 2.

$\gamma > \gamma^*$: For these large γ values, the chaotic fluctuations are too violent to allow periodic behavior: For L's larger than roughly 50 the amplitude of the oscillations in $M(t)$ decreases with L, as illustrated in Fig. 5. The resulting steady state is not scale invariant: the susceptibility saturates with L (Fig. 2), though, again, only at fairly large sizes ($L \approx 50$ for $\gamma = 2$), and $P(s)$, shown for $\gamma = 1.99$ in Fig. 6, is consistent with exponential decay with a characteristic avalanche size $s_0 \approx 350$, independent of L. We believe that the relatively long correlation lengths reflected in the large values of L required for saturation are responsible for the attribution of SOC to the earlier data collected at finite p. We have taken susceptibility data at small positive p which show the susceptibility achieving a maximum at $p \approx 0.003$ (Fig. 7), and then *decreasing* with decreasing p, consistent with our results at $p = 0$. We also note that care must be taken at $\gamma = 2$ to avoid drastic artifacts of binary computation. This is the reason we quote results for $\gamma = 1.99$ rather than exactly 2.

V. STICK-SLIP MODELS

Definition

Again a real variable u_i is defined on each site of an $L \times L$ lattice with periodic boundary conditions and random initial conditions. The u_i's are increased at a uni-

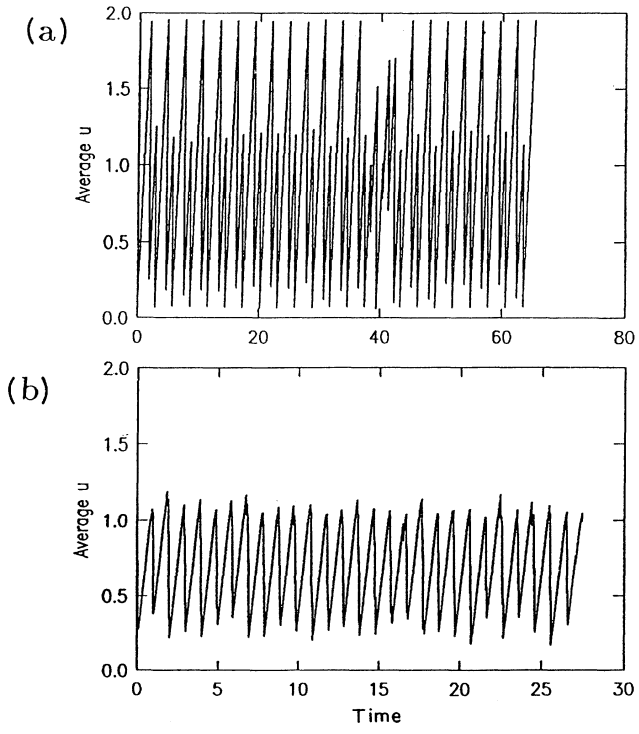

FIG. 3. Mean variable value $M(t)$ as a function of time t for the FFM with $\gamma = 1.1$ and periodic boundary conditions, illustrating the two different states periodic in the mean: (a) $L = 16$; (b) $L = 64$.

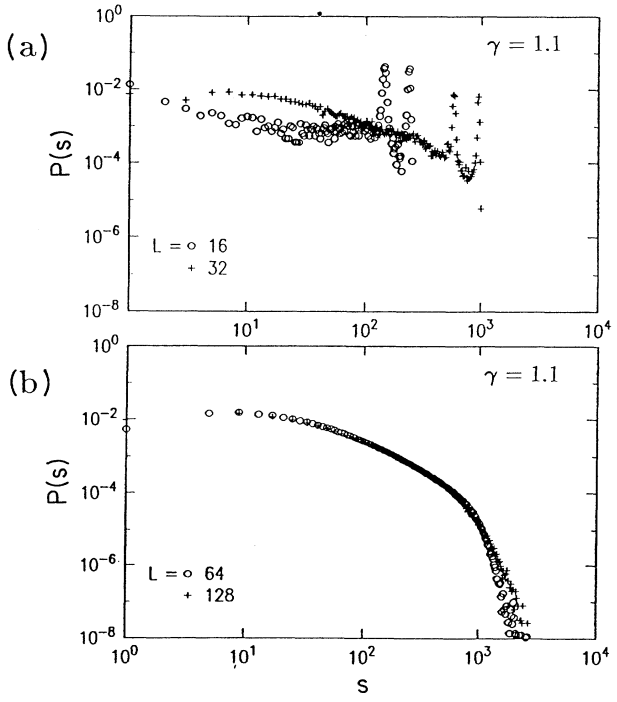

FIG. 4. Avalanche size distributions for the FFM with $\gamma = 1.1$ in the two types of states that are periodic in the mean: (a) $L = 16$ and 32 (approximately 10^4 avalanches each); (b) $L = 64$ and 128 (approximately 10^6 avalanches each). For clarity, the points shown are averages over a bin, where the horizontal logarithmic scale is partitioned into 500 equal width bins.

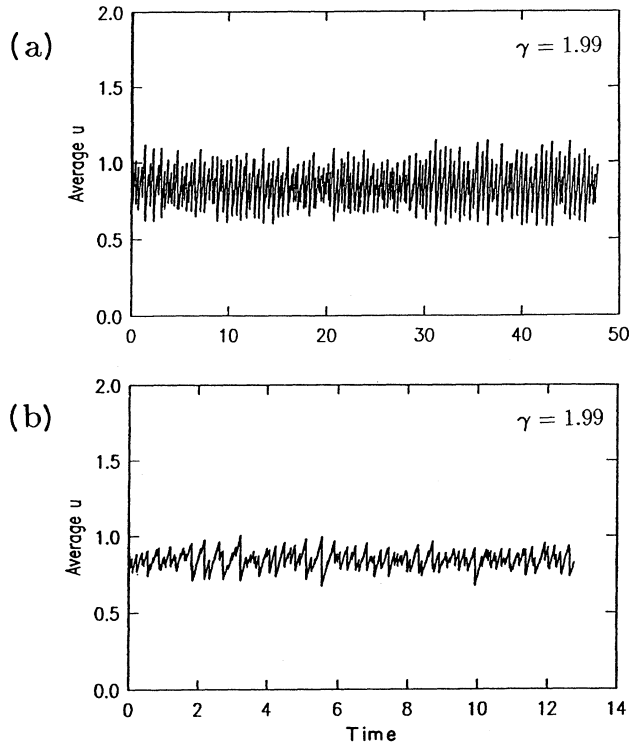

FIG. 5. Mean variable value $M(t)$ as a function of time t for the FFM with $\gamma=1.99$ and periodic boundary conditions: (a) $L=32$; (b) $L=64$. Note the clear decrease in the strength of the oscillations with increasing L.

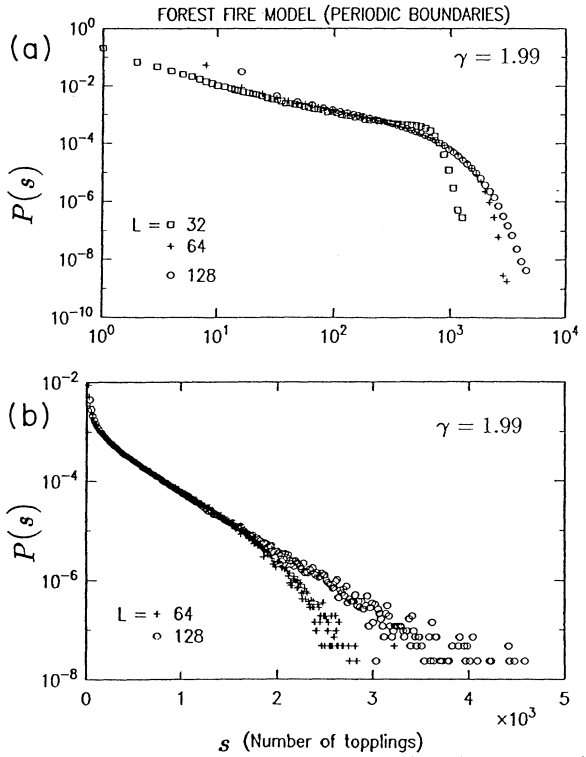

FIG. 6. Avalanche size distributions for the FFM with $\gamma=1.99$ and $L=32$, 64, and 128 (approximately 3×10^6 avalanches each). (a) log-log plot; (b) log-linear plot. Note the exponential decay for large L.

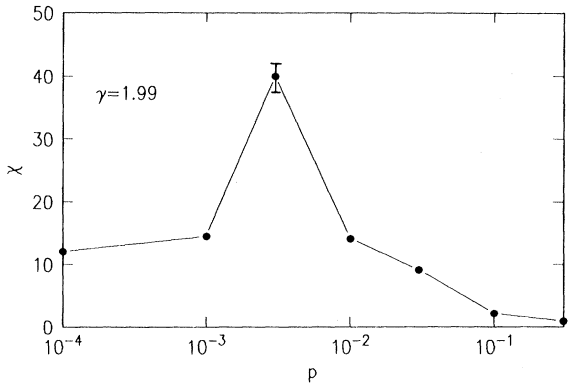

FIG. 7. Susceptibility as a function of driving rate for the FFM with $\gamma=1.99$. Values shown are the saturation values of χ at large L. The point at $p=0.003$ is somewhat uncertain, as indicated. At this p, clear saturation did not occur for L's up to 128, and extrapolation of data from smaller L's was necessary.

form rate until one of them reaches a specified threshold U and initiates an avalanche, which consists of a sequence of synchronous updates of the lattice. At each step, any unstable site $u_i > U$ topples: $u_i \to 0$. Simultaneously, any $u_j < U$ that is the nearest neighbor of one or more unstable sites is kicked: $u_j \to \gamma u_j + \alpha \sum_i u_i$, where α and γ are real parameters and the sum runs over the unstable nearest neighbors of u_j. The avalanche stops when all sites are stable, and the continuous driving resumes.

When $\gamma=1$, this model is, apart from boundary conditions, the one studied in Ref. [8]. There u_i represents the total elastic force on a block in a block-spring model of a fault. Each block rests on a frictional surface and is connected by springs to its nearest neighbors and to a rigid plate that is assumed to move at a very slow constant velocity. The toppling and kicking rules approximate the redistribution of stress occurring when the force on a block, which increases as the rigid plate moves, overcomes static friction. In Ref. [8], the distribution of avalanche sizes $P(s)$ is numerically computed for $0.05<\alpha<0.25$, where s is defined to be the number of topplings in an avalanche. The fact that $P(s)$ decays algebraically is interpreted as evidence for SOC. The data indicate that the exponent governing the decay varies with α, with $P(s)\sim s^{-1.91}$ at $\alpha=0.2$. It is also argued that $\alpha=0.2$ is a physically relevant value.

We note that the driving, toppling, and kicking rules used in Ref. [8] were derived under the assumption that all of the springs in the system are perfectly linear. A striking consequence of this assumption is that the sizes of the kicks and the rate of increase between the kicks do not depend in any way on the position of a block relative to its neighbors and the rigid plate. Nonlinearities in the springs, no matter how small, would alter this situation and therefore must be considered. To incorporate the effects of nonlinearities in detail would complicate the model considerably. Instead, by allowing $\gamma\neq1$, we introduce in the simplest way terms in the dynamics that allow the change in u_i to depend on the value of u_i at a site that is kicked even when the kick does not put the site

over threshold. The point is that, among other effects, the nonlinear terms in the elasticity remove a certain degeneracy in the system, so a system possessing that degeneracy cannot be considered generic. Setting $\gamma \neq 1$ is the simplest way of removing the degeneracy and hence of avoiding artifacts associated with it, though it does not model the elastic nonlinearities in detail. The observed qualitative changes in the behavior for different γ's suggest that the linear model is not, in fact, representative of a generic physical system.

We have simulated the SSM for $\alpha = 0.2$ and a range of γ. We characterize the steady states by their avalanche statistics and Lyapunov exponents, computed as in the FFM. When periodic boundary conditions are applied, there are four regimes of qualitatively different behavior.

(i) $\gamma \leq 1-\alpha$: Only $s=1$ avalanches are possible since $\gamma u + \alpha U < U$ for any $u < U$. After a short transient (~ 10 cycles), a periodic state with $T=1$ is reached. Though $\lambda(\gamma;L)$ varies slightly from run to run, it is always negative and decreases in magnitude for increasing L. For example, averaging over four runs for each case, we find $\lambda(0.799;8) \approx -1.3\times10^{-1}$, $\lambda(0.799;16) \approx -3\times10^{-2}$, and $\lambda(0.799;32) \approx -7\times10^{-3}$.

(ii) $1-\alpha < \gamma < 1$: Here too the system always settles into a periodic state with $\lambda < 0$. As above, $|\lambda|$ decreases as L increases, though λ varies slightly from run to run. There is also a clear decrease in $|\lambda|$ as γ is increased toward 1; $\lambda(0.9;16) \approx -2\times10^{-2}$ and $\lambda(0.99;16) \approx -2\times10^{-3}$. In this regime, avalanches with $s>1$ can and do occur, with an increasing proportion of large ones as γ increases. Figure 8(a) shows distributions for $\gamma = 0.9$ and 0.95 averaged over 500 periodic states. Periods $T>1$ also occur more frequently as γ increases, though $T=1$ remains the most probable for all γ's we have examined, which include values up to 0.99. As γ approaches 1, the transients leading to the periodic states become extremely long.

(iii) $\gamma > 1$: In this case, one finds states for which $P(s)$ is nonzero only at a few different values of s, some of which are close to L^2. Most of these states are periodic with small period, but in some the sequence in which different size avalanches occur appears chaotic. By far the most common states are periodic with a cycle consisting of a single avalanche of size L^2. [See Fig. 8(b).] Periodic states with $T>1$ are also possible: we have observed periods of up to 62 cycles (always with $\lambda<0$). Note that if γ is made sufficiently large, the toppling and kicking rules result in a net *increase* of u and an avalanche of infinite duration is produced. All our simulations are done below this regime, which would be expected to start in the vicinity of $\gamma = 1+(1-4\alpha)/2$, the point where a typical toppling event (in which the average u of the kicked sites is $U/2$) just conserves the total u.

(iv) $\gamma = 1$: Remarkably, this special case displays completely different behavior from either the complex periodic states at $\gamma = 1^-$ or the periodic states with $s=L^2$ at $\gamma = 1^+$, all of which have $\lambda<0$ and some (or all) large avalanches. For $\gamma=1$, the system rapidly settles into a periodic state with $T=1$, all $s=1$ avalanches, and $\lambda=0$. These states are truly marginal: the stable state changes continuously with small changes in initial conditions.

A partial understanding of the above observations can be obtained from the analysis of a system consisting of just two sites. Letting x_n denote the value of u_1 immediately after the nth toppling of u_2, we construct the return map shown in Fig. 9. For $\gamma<1$ there is an attractive

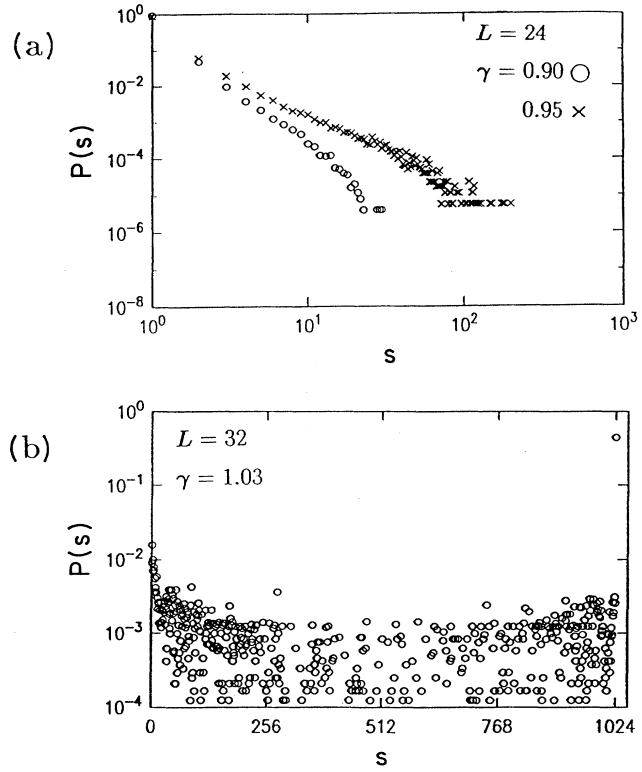

FIG. 8. Avalanche size distributions for the SSM with periodic boundary conditions and $\alpha = 0.2$. Data are averaged over 500 periodic states obtained from different random initial conditions. Each individual run gives only a few distinct s values. (a) $\gamma = 0.90$ and 0.95; note that 90% of the events have $s=1$. (b) $\gamma > 1.03$; note the frequent occurrence of $s=L^2$.

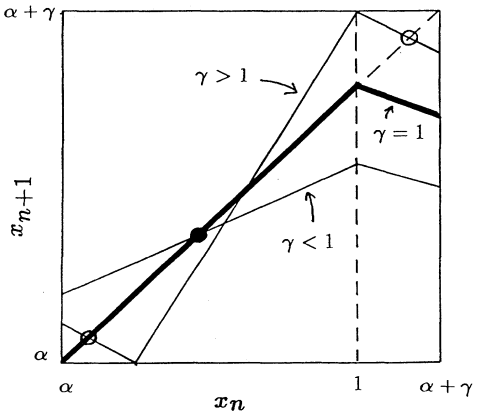

FIG. 9. Return map for the two-site SSM. The solid circle marks the stable fixed point for $\gamma<1$. For $\gamma>1$, the open circles mark the stable fixed points, in which both sites topple in the same avalanche. The segment of the thick line lying on the diagonal, $x_{n+1}=x_n$, is the set of marginal fixed points for $\gamma=1$. The axes are marked in units where the threshold U is unity.

fixed point corresponding to a state where the sites oscillate exactly out of phase and every avalanche has $s=1$. For $\gamma>1$ this fixed point is unstable, but a different stable fixed point exists corresponding to a synchronous state in which both sites topple in the same avalanche. $\gamma=1$ is unique is that there is no preferred phase relation for the two sites, but rather a continuous range of marginally stable ones. Thus for the two-site system the differences between the regimes $\gamma<1$, $=1$, and >1 mirror the observed differences in the extended system. It is also worth noting that a similar analysis of the FFM reveals no analog of the synchronous fixed point for $\gamma>1$, so that even the two-site system is chaotic.

A full generalization of this analysis, including a complete characterization of the periodic states, is beyond the scope of this work. Some simple arguments can be made, however, regarding the crucial feature of whether or not the periodic states of the extended system have $\lambda=0$. We show analytically in the Appendix that the periodic states reached for $\gamma\neq1$ are insensitive to small perturbations: the states are not marginal. The numerics confirm this analysis and, in fact, show that λ is strictly negative.

Since all the stable states are either strictly periodic (with $\lambda<0$) or have manifestly noncritical avalanche distributions, there is no SOC in the SSM with periodic boundary conditions.

VI. REMARKS ON OPEN BOUNDARY CONDITIONS

We have seen that with periodic boundary conditions neither the FFM nor the SSM exhibits SOC for any γ, including the value $\gamma=1$ with which the models were originally defined. At this special value, however, both models exhibit unique properties connected with the vanishing of the maximum Lyapunov exponent.

One is naturally led to ask whether the numerical evidence [in $P(s)$ data [8]] for SOC at $\gamma=1$ in the SSM with *open* boundary conditions is likewise a unique feature or whether it survives for some range of γ. It is difficult to answer this question purely on the basis of numerics, particularly numerics for the avalanche size distribution alone. For $\gamma=0.90$, Fig. 10(a) shows $P(s)$ cutting off at a value $s^*\sim10$, which is independent of L; there is no scale invariance. For $\gamma=0.95$, however, $P(s)$ has a small tail which moves out to larger s values with increasing L [Fig. 10(b)], possibly indicative of scale-invariant behavior. It is hard to decide whether these data imply a divergence of the correlation length for γ somewhere between 0.90 and 0.95, and hence generic SOC, or a correlation length at 0.95 that is comparable to the largest sample sizes but finite, diverging only at $\gamma=1$. (Recall that in the FFM correlation lengths even in the strongly chaotic region near $\gamma=2$ were 50 or more, with characteristic avalanche sizes of 350.) Data for γ slightly greater than 1 are similarly ambiguous; $P(s)$ certainly looks algebraic at $\gamma=1.02$, for example, as shown in Fig. 10(c).

Susceptibility and Lyapunov exponent data shed some light on this conundrum. At both $\gamma=1.02$ and 1.00, χ appears to grow like L^2 out to $L=128$, i.e., over the entire range of L for which algebraic behavior of $P(s)$ has been observed. Correspondingly, $M(t)$ shows oscillations (Fig. 11) which do not decrease appreciably with L. Thus for γ equal to or slightly greater than 1, the power-law decays of $P(s)$ are associated with apparently chaotic oscillations in the mean, i.e., with a breaking of time-translation invariance and the presumed concomitant Goldstone mode. At $\gamma=1.02$ with open boundary conditions we also find λ to be positive, as in the FFM for $\gamma>1$, while at $\gamma=1.00$ λ is indistinguishable from zero.

These results admit two obvious possibilities for behavior consistent with scale-invariant decay of $P(s)$ in the large-L limit: (1) The symmetry-breaking oscillations

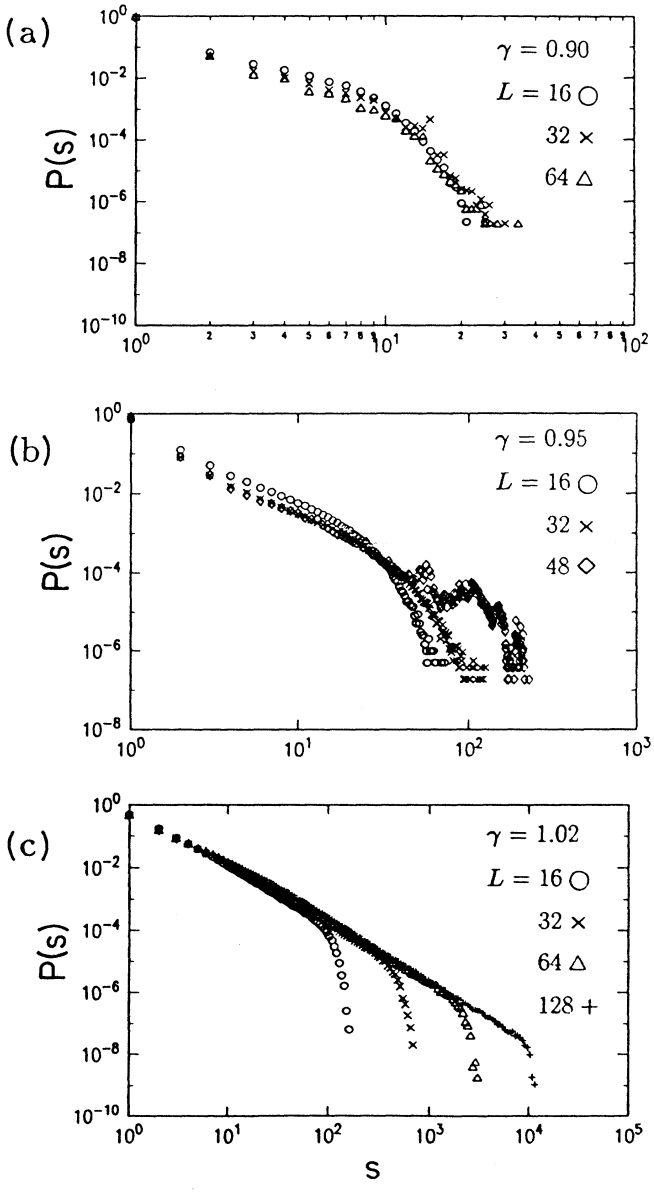

FIG. 10. Avalanche size distributions for the SSM with open boundary conditions and $\alpha=0.2$. Data correspond to a single state and include approximately 4×10^6 avalanches in each case. Note the differences in the horizontal scales. (a) $\gamma=0.90$; note the lack of change in the distribution with increasing L and the similarity with the periodic boundary condition case [Fig. 8(a)]. (b) $\gamma=0.95$; again note the similarity with Fig. 8(a). (c) $\gamma=1.02$; these data look scale invariant, differing markedly from Fig. 8(b).

in the mean persist, perhaps becoming truly periodic at large L; whether one calls this SOC or not is, as discussed earlier, a matter of definition. (2) The oscillations disappear but the algebraic $P(s)$ survives; this would be "conventional" SOC providing it occurs over a range of γ and not just at $\gamma=1$, where λ apparently vanishes. Of course the scale invariance in $P(s)$ could simply fail to survive at large L, a failure that might be accompanied either by the disappearance of the oscillations or by their persistence (recall the FFM for $1<\gamma<\gamma^*$). Clearly it is difficult to identify the correct scenario without more data. Our goal here is merely to point out that even for the special point $\gamma=1$ there does not yet exist any numerical evidence for scale invariance of $P(s)$ in the absence of macroscopic temporal oscillations. Scale invariance without symmetry breaking for a nonzero range of γ is still more problematic.

For $\gamma<1$, where there is no evidence of macroscopic oscillations, χ values are two orders of magnitude lower at $\gamma=0.95$ than at $\gamma=1.02$, consistent with the weakness of the tail in $P(s)$. We cannot, however, rule out the possibility that χ increases indefinitely with L. More significant, perhaps, is that preliminary measurements show λ to be negative. This suggests that the stable states of the system may in fact be strictly periodic, and that one is observing either long transients or states with extremely long periods. (Of course the same possibility exists even for $\gamma>1$, but there the possibility of trajectory spreading in the kicking rule makes chaotic states seem more likely.) Strictly periodic behavior would be similar to what we observed with periodic boundary conditions for $1-\alpha<\gamma<1$. Indeed, a hint of the tail in the $P(s)$ data for $\gamma=0.95$ and open boundaries can be found in the SSM with periodic boundary conditions: If one averaged $P(s)$ over many different stable states one obtains (Fig. 8) a rather similar tail. Given the marked effect of boundary conditions on the behavior of the SSM for $\gamma\geq 1$, we hesitate to infer that only periodic states without scale invariance occur for $\gamma<1$ and open boundaries. It is worth mentioning, however, that for very small systems ($L\leq 6$, say), periodic states do occur at $\gamma=0.95$ with open boundaries, after long transients. Though transients that persist for sufficiently long times can be as relevant as asymptotic behavior, complete understanding requires the correct identification of transient and asymptotic phenomena.

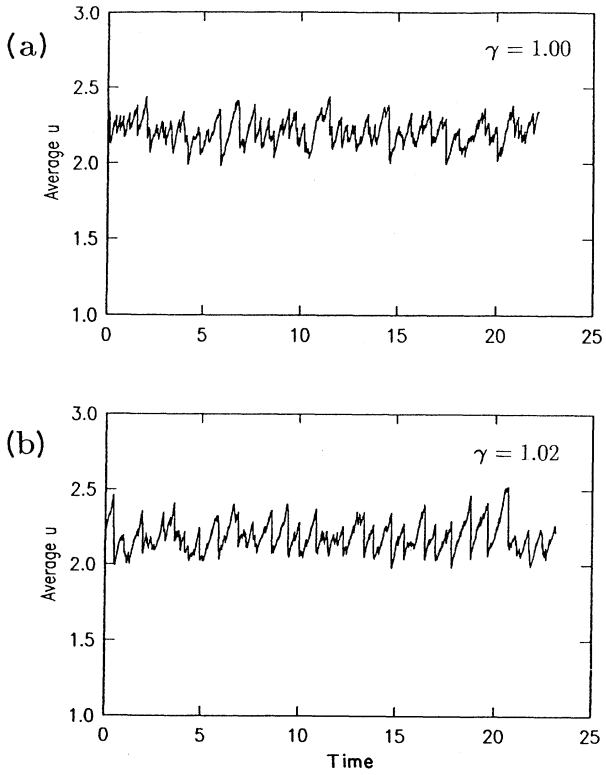

FIG. 11. Mean variable value $M(t)$ as a function of time t for the SSM with $L=32$ and open boundary conditions: (a) $\gamma=1$; (b) $\gamma=1.02$.

Finally, it is interesting to speculate about the origin of the powerful effect of boundary conditions on systems like the SSM. Naively one might expect that, unlike in conserving systems in which transport of the conserved quantity to a boundary can be necessary to maintain a steady state [5,22], noncritical nonconserving systems should be relatively insensitive to boundaries. We conjecture that the tendency of the SSM towards periodic behavior is responsible for the observed sensitivity. We have seen that with periodic boundary conditions this model readily finds regular periodic states in which all sites cycle at the same frequency. With open boundaries, where the boundary sites have fewer neighbors and so are kicked less often, different sites must cycle at different frequencies. While the system might interpolate somehow between surface and bulk sites in a finite boundary layer, it is possible that the boundary acts as a permanent source of perturbations which disrupt the order arbitrarily far away. The present work provides an appropriate context for further study of this issue.

Note added in proof. Since the submission of this paper, we have become aware of a forest-fire model with *two* sets of infinitely separated time scales that has been argued to exhibit SOC without a conservation law. See C. L. Menley (unpublished); and B. Drossel and F. Schwabl, Phys. Rev. Lett. **69**, 1629 (1992).

ACKNOWLEDGMENTS

We thank J. Krug for extensive helpful conversations. C.J. acknowledges financial support from the U.S. Department of Energy, Office of Basic Energy Sciences (Grant No. DE-FG02-88ER13916); he is also grateful to the Ohio Supercomputer Center for providing a grant of computer time.

APPENDIX: STABILITY OF PERIODIC STATES OF THE SSM

For any given toppling order in a periodic state, we show that there is a unique solution for the values of u_i. Consider first a state with $T=1$ and only $s=1$ avalanches and let z be the number of nearest neighbors of each site. (For the square lattice $z=4$.) The time evolution of site i is conveniently specified by $z+2$ quantities: ϕ_i, the time

during the cycle at which site i topples; and $t_i^{(k)}$ with $k=1,\ldots,z+1$, where $t_i^{(1)}$ is the time interval between the toppling of site i and the first kick it receives from a neighbor, $t_i^{(2)}$ is the interval between the first kick and the second, etc., and t_i^{z+1} is the interval between the last kick from a neighbor and the next toppling of site i. We take the ramping speed due to continuous driving to be U, so the increase in u during time t is Ut. We may also define $\phi_i=0$ for one particular site without loss of generality. The $T=1$ periodic state with all $s=1$ is thus specified by $(z+2)N-1$ variables, where N is the total number of sites. These must satisfy the following independent linear equations.

The total time for each site's oscillation must be the same:

$$\sum_{k=1}^{z+1} t_i^{(k)} = \sum_{k=1}^{z+1} t_j^{(k)} \tag{A1}$$

for all i and j. These are $N-1$ independent equations.

Each site must reach $u_i=U$ at the end of t_i^{z+1}:

$$\sum_{k=1}^{z+1} \gamma^{z+1-k} t_i^{(k)} + \alpha \sum_{k=0}^{z-1} \gamma^k = 1 \ . \tag{A2}$$

These are N independent equations.

The time between the toppling of u_i and its next kick from a particular neighbor u_j must equal the time between the toppling of u_j and its previous kick from the toppling of u_i:

$$\sum_{k=1}^{x} t_i^{(k)} = \sum_{k=y}^{5} t_j^{(k)} \ , \tag{A3}$$

where x and y are determined by the toppling order of the particular state in question. There is one such equation for each nearest-neighbor bond, for a total of $Nz/2$ independent equations.

The relative phases of two neighboring sites must be consistent with the time intervals:

$$\phi_i - \phi_j = \sum_{k=1}^{x} t_j^{(k)} \ , \tag{A4}$$

where ϕ_i is taken to be the larger of the two phases and x corresponds to the toppling of site i. These are $Nz/2$ independent equations.

Since we have the same number of independent linear equations as unknowns, there is only one solution. This implies that the states under consideration are stable against small perturbations.

This reasoning can be extended in a straightforward way to $T=1$ periodic states that include avalanches with $s>1$. For those sites that are kicked over threshold in an avalanche, one simply replaces the variable ϕ_i, which is now fixed at the phase of the site initiating the avalanche, by the variable r_i that measures the height to which it is kicked. In addition, for each such kick $t_i^{(1)}=t_j^{(5)}=0$, where i indicates the kicking site and j the kicked site. Equation (A2) must be modified to account for the fact that $r_i \neq 1$, but remains linear. The appropriate bookkeeping then reveals that the number of variables and the number of equations match, as before. The numerical results indicate that appropriate generalization to periodic states with $T>1$ would yield the same result.

The above argument breaks down for $\gamma=1$. In this case, Eqs. (A1) and (A2) become redundant, leaving the system underdetermined. The system has a zero Lyapunov exponent for each undetermined degree of freedom. Thus $\gamma=1$ is seen to be a unique critical point in the sense that $\lambda(1;L)=0$ for $T=1$ periodic states. Though for $\gamma=1$ one can construct states with large avalanches quite easily, it can be shown that they only arise for fine-tuned initial configurations in which some neighboring sites differ by exactly α, so in practice one sees only the simplest periodic states with $s=1$ for all avalanches.

---

*Present address: Physics Department, Duke University, Durham, NC 20776.

[1] P. Bak, C. Tang, and K. Wiesenfeld, Phys. Rev. Lett. **59**, 381 (1987).

[2] P. Bak and K. Chen, Physica D **38**, 5 (1989).

[3] T. Hwa and M. Kardar, Phys. Rev. Lett. **62**, 1813 (1989); P. L. Garrido, J. L. Lebowitz, C. Maes, and H. Spohn, Phys. Rev. A **42**, 1954 (1990); G. Grinstein, J. Appl. Phys. **69**, 5441 (1991).

[4] D. Dhar, Phys. Rev. Lett. **64**, 1613 (1990).

[5] L. P. Kadanoff, S. R. Nagel, L. Wu, and S. M. Zhou, Phys. Rev. A **39**, 6524 (1989).

[6] K. Chen, P. Bak, and M. H. Jensen, Phys. Lett. A **149**, 207 (1990).

[7] H. J. S. Feder and J. Feder, Phys. Rev. Lett. **66**, 2669 (1991).

[8] Z. Olami, H. J. S. Feder, and K. Christensen, Phys. Rev. Lett. **68**, 1244 (1992).

[9] Both the FFM and SSM (as we define them) differ from the Abelian sandpile models is that the variables are real rather than integers, and the driving is continuous and deterministic. All sites are increased at a uniform rate until one reaches threshold and initiates an avalanche. The avalanche rules are also non-Abelian: the order in which avalanches occur is important. In the Abelian models, the variables take on only integer values, and the driving is accomplished by incrementing randomly selected sites. The avalanche dynamics are such that the state of the system does not depend on the order in which the sites are incremented.

[10] By "stable" states we mean the states or attractors achieved by the system after transients have decayed. When there is multistability, i.e., different states are reached from different initial conditions, we refer to all the achievable states as "stable," making no attempt to decide their relative stability.

[11] T. Bohr, G. Grinstein, Y. He, and C. Jayaprakash, Phys. Rev. Lett. **58**, 2155 (1987).

[12] J. Crutchfield and K. Kaneko, in *Directions in Chaos*, edited by B.-L. Hao (World Scientific, Singapore, 1987), Vol. 1.

[13] See, e.g., D. Forster, *Hydrodynamic Fluctuations, Broken*

Symmetry, and Correlation Functions (Benjamin, Reading, MA, 1975).

[14] S. P. Obukhov, Phys. Rev. Lett. **65**, 1395 (1990), discusses Goldstone modes in the context of SOC, but does not consider broken time-translation symmetry.

[15] While we discuss the evolution of the system in terms of a continuous time variable, for some purposes a discrete time variable may be appropriate; e.g., each update of the lattice might be considered a unit time step. Strictly speaking, the time-translation symmetry is fully broken only if the period of the macroscopic oscillations is an irrational number of discrete time steps, which we believe to be the case in the systems studied here. Note that these systems differ from those studied in Ref. [11] in that the rule requiring that all evolution at distant sites stop while an avalanche is carried out represents an effective long-range interaction.

[16] J. M. Kosterlitz and D. J. Thouless, J. Phys. C **6**, 1181 (1973); J. M. Kosterlitz, *ibid.* **7**, 1046 (1974).

[17] Chen, Bak, and Jensen, Ref. [6], have argued from numerics performed at small positive p that the maximum Lyapunov exponent for the forest-fire model at $\gamma=2$ is zero, and that trajectories spread algebraically. We believe that this conclusion is an incorrect consequence of using time intervals that were too short—smaller than the cycle time $1/p$, in fact. Unless one computes λ by monitoring many cycles and using the cycle time as the basic time unit one can erroneously conclude that $\gamma=0$ as p gets small, simply because the kicking processes that cause trajectories to diverge when $\gamma>1$ only occur with frequency $1/p$, roughly. Taking the cycle time as the basic time unit, we have found $\lambda>0$ for $\gamma>1$ both for small p and $p=0$.

[18] Certain 1D models treated in Ref. [5] require multiscaling rather than straightforward finite-size scaling to fit the data. See J. Krug, J. Stat. Phys. **66**, 1635 (1992).

[19] K. Binder and A. P. Young, Rev. Mod. Phys. **58**, 801 (1986).

[20] See, e.g., P. Bak, K. Chen, and C. Tang, Phys. Lett. A **147**, 297 (1990); and P. Grassberger and H. Kantz, J. Stat. Phys. **63**, 685 (1991), for discussions of a related stochastic forest-fire model.

[21] J. M. Carlson and J. S. Langer, Phys. Rev. Lett. **62**, 2632 (1989); T. Hwa and M. Kardar, Phys. Rev. A **45**, 7002 (1992).

[22] J. M. Carlson, J. T. Chayes, E. R. Grannan, and G. H. Swindle, Phys. Rev. Lett. **65**, 2547 (1990); J. Krug, Ref. [18].